Condensation phase transitions of symmetric conserved-mass aggregation model on complex networks

Sungchul Kwon, Sungmin Lee, and Yup Kim*

Department of Physics and Research Institute for Basic Sciences, Kyung Hee University, Seoul 130-701, Korea
(Received 16 December 2005; published 3 May 2006)

We investigate condensation phase transitions of the symmetric conserved-mass aggregation (SCA) model on random networks (RNs) and scale-free networks (SFNs) with degree distribution $P(k) \sim k^{-\gamma}$. In the SCA model, masses diffuse with unit rate, and unit mass chips off from mass with rate ω. The dynamics conserves total mass density ρ. In the steady state, on RNs and SFNs with $\gamma > 3$ for $\omega \neq \infty$, we numerically show that the SCA model undergoes the same type of condensation transitions as those on regular lattices. However, the critical line $\rho_c(\omega)$ depends on network structures. On SFNs with $\gamma \leq 3$, the fluid phase of exponential mass distribution completely disappears and no phase transitions occurs. Instead, the condensation with exponentially decaying background mass distribution always takes place for any nonzero density. For the existence of the condensed phase for $\gamma \leq 3$ at the zero density limit, we investigate one lamb-lion problem on RNs and SFNs. We numerically show that a lamb survives indefinitely with finite survival probability on RNs and SFNs with $\gamma > 3$, and dies out exponentially on SFNs with $\gamma \leq 3$. The finite lifetime of a lamb on SFNs with $\gamma \leq 3$ ensures the existence of the condensation at the zero density limit on SFNs with $\gamma \leq 3$, at which direct numerical simulations are practically impossible. At $\omega = \infty$, we numerically confirm that complete condensation takes place for any $\rho > 0$ on RNs. Together with the recent study on SFNs, the complete condensation always occurs on both RNs and SFNs in zero range process with constant hopping rate.

I. INTRODUCTION

Nonequilibrium condensation phase transitions from fluid phase into condensed phase have been observed in a variety of phenomena ranging from traffic flow to polymer gels [1–13]. In the steady state, a finite fraction of total particles condenses on a single site in the condensed phase when the total particle density ρ is increased beyond a certain critical value ρ_c. In the fluid phase below ρ_c, the particle number of each site fluctuates around ρ without the condensation.

Various kinds of nonequilibrium mass transport models exhibit the condensation transitions or only condensation. The simplest and well-known model is the zero-range process (ZRP) in one dimension [1]. In ZRP, many identical particles occupy sites on a lattice. Each site may contain an integer number of particles and one of these particles can hop to one of the nearest-neighboring sites with a rate that depends on the number of particles at the site of departure. The chipping (single-particle dissociation) and aggregation processes of ZRP describe various condensations, such as jamming of traffic [2], bunching of buses [3], coalescence of shaken steel balls [4], and condensation of edges in networks [5]. Recent studies of ZRP on scale-free [6] and directed networks [7] reveal the conditions under which condensation takes place.

Another important class of condensation transitions emerges when the diffusion of the whole particles of a single site is involved in addition to the chipping and aggregation. These processes arise in a variety of phenomena such as polymer gels [8], the formation of colloidal suspensions [9],

river networks [10,11], and clouds [12]. The recently studied conserved-mass aggregation (CA) model is the simplest one incorporating diffusion, chipping, and aggregation upon contact [13,14]. In the one-dimensional CA model, the mass m_i of site i moves either to site $i-1$ or to site $i+1$ with unit rate, and then $m_i \to 0$ and $m_{i\pm1} \to m_{i\pm1} + m_i$. With rate ω, unit mass chips off from site i and moves to one of the nearest-neighboring sites; $m_i \to m_i - 1$ and $m_{i\pm1} \to m_{i\pm1} + 1$. As total masses are conserved, the conserved density ρ and ω determine the phase of the CA model. The condensation transition arises via the competition between diffusion and chipping processes. The diffusion of masses tends to produce massive aggregates and consequently creates more vacant sites. The chipping of unit mass tends to prevent the formation of aggregates, so that it leads to a replenishment of the lower end of mass distribution.

The single site mass distribution $P(m)$, i.e., the probability that a site has mass m in the steady state, was shown to undergo phase transitions on regular lattices [13]. For a fixed ω, as ρ is varied across the critical value $\rho_c(\omega)$, the behavior of $P(m)$ for large m was found to be [13]

$$P(m) \sim \begin{cases} e^{-m/m^*}, & \rho < \rho_c(\omega) \\ m^{-\tau}, & \rho = \rho_c(\omega) \\ m^{-\tau} + \text{infinite aggregate}, & \rho > \rho_c(\omega), \end{cases} \quad (1)$$

where ρ_c is given as $\rho_c(\omega) = \sqrt{\omega+1} - 1$. ρ_c and τ are shown to be independent of spatial dimension d [14]. The tail of the mass distribution changes from exponential to an algebraic decay as ρ approaches ρ_c from below. As one further increases ρ beyond ρ_c, this asymptotic algebraic part of the critical distribution remains unchanged, but in addition an

infinite aggregate forms. This means that all the additional mass $(\rho-\rho_c)L^d$ condenses onto a single site and does not disturb the background critical distribution. The $\omega=\infty$ case corresponds to ZRP with constant chipping rate, and then there is no condensation transitions on regular lattices. The critical exponent τ is the same everywhere on the critical line $\rho_c(\omega)$. Recent studies showed that τ depends on the symmetry of movement and constraints of diffusion rate [15,16]. In what follows, we only consider the symmetric CA (SCA) model, where diffusion and chipping directions are unbiased [13].

As mean-field theory correctly predicts the phase diagram and τ of the SCA model in one dimension [13], the nature of the condensation transitions should remain unchanged in any higher dimensions. However, recent studies of various dynamics on network structures showed that the structure of networks leads to more rich and intriguing behavior different from that predicted by the standard mean-field theory on regular lattices [5,6,17]. For example, ZRP on SFNs was shown to exhibit condensation even at constant hopping rate, which is the case of an infinite chipping rate of the SCA model [6].

In this paper, we investigate the effect of network structures on the condensation transitions of the SCA model using random networks (RNs) and scale-free networks (SFNs). As we shall see, on RNs and SFNs with the degree exponent $\gamma>3$, the SCA model undergoes the same type of condensation transitions as those in a regular lattice across a critical line $\rho_c(\omega)$ in the ρ-ω plane with the exponent $\tau=5/2$. However, on SFNs with $\gamma\leqslant3$ where one or several nodes, so-called hub nodes, have a finite fraction of links, the fluid phase completely disappears and the condensation with exponentially decaying background mass distribution takes place for any nonzero density. The outline of this paper is as follows. In Sec. II, we introduce the SCA model on complex networks. The condensation transitions on RNs and SFNs are discussed in Secs. III and IV. To understand the condensation on SFNs with $\gamma\leqslant3$, we discuss lamb-lion problems on SFNs in Sec. V. In Secs. VI and VII, we discuss the SCA model at $\omega=\infty$ and the effect of diffusion of masses on average mass distribution on degrees, respectively. Finally, we summarize our results in Sec. VIII.

II. SCA MODEL ON NETWORKS

We consider a network with N nodes and K links. The degree k_i of a node i is defined as the number of its links connected to other nodes. The average degree of a node $\langle k\rangle$ is given as $\langle k\rangle=2K/N$. The degree distribution $P(k)$ is a Poisson distribution for RNs and a power-law distribution of $P(k)\sim k^{-\gamma}$ for SFNs. Each node may have an integer number of particles, and the mass of a node is defined as the number of particles at the node. Initially M particles randomly distribute on N nodes with given conserved density $\rho=M/N$. Next a node i is chosen at random and one of the following events occurred:

(i) Diffusion: With unit rate, the mass m_i moves to the randomly selected nearest-neighboring node j. If the node
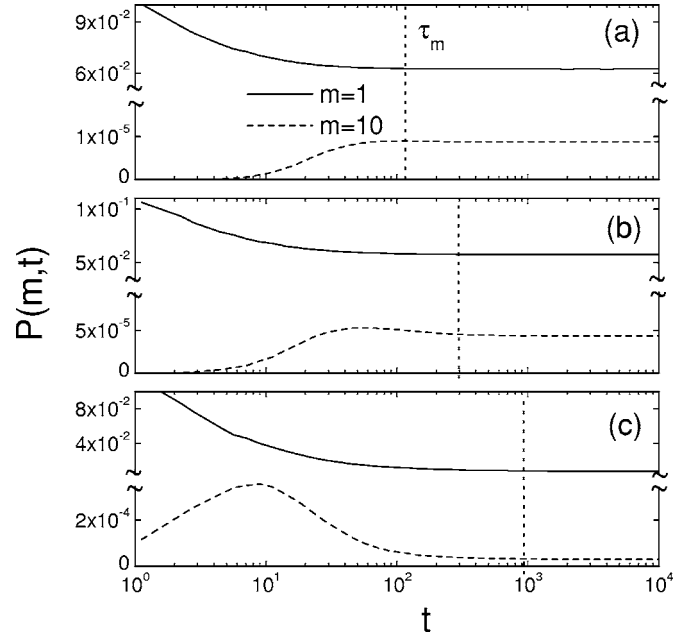

FIG. 1. $P(m,t)$ of $m=1$ and 10 for $\rho=0.2$ and $\omega=1$ on networks of $N=10^4$. Each panel corresponds to RN (a), SFN with $\gamma=4.3$ (b), and $\gamma=2.4$ (c). The vertical dotted line denotes the characteristic time τ_m.

j already has mass m_j, then the aggregation takes place; $m_i\rightarrow0$ and $m_j\rightarrow m_j+m_i$.

(ii) Chipping: With rate ω, unit mass (a single particle) at node i chips off and moves to the randomly selected nearest-neighboring node j; $m_i\rightarrow m_i-1$ and $m_j\rightarrow m_j+1$.

As mentioned in Sec. I, diffusion and chipping processes compete with each other so a condensation transition physically depends on two external parameters ρ and ω. At $\omega=0$, however, only diffusion and aggregation take place so masses always condense onto a single site (complete condensation). On the other hand, the $\omega=\infty$ case corresponds to ZRP with constant chipping rate. It was shown that ZRP on scale-free networks exhibits complete condensation when the mass-dependent chipping rate $u(m)$ is given as $u(m)\sim m^\delta$, but $\delta<\delta_c$, where δ_c is some threshold value [6]. Hence the SCA model of $\omega=\infty$ is just the $\delta=0$ case of ZRP so the complete condensation always arises at $\omega=\infty$. As we shall see in the following section, the complete condensation for ZRP also takes place on random networks at $\rho>0$.

For the construction of SFN, we use a static model [18] instead of preferential attachment algorithm [5]. In the static model, it is desired to use large $\langle k\rangle$ to construct fully connected networks. In simulations, we use $\langle k\rangle=4$.

III. SCA MODEL ON RNs AND SFNs WITH $\gamma>3$

We consider the SCA model on RNs and SFNs with $\gamma>3$ having nodes $N=10^4$ and links $K=2\times10^4$ for $\omega\neq\infty$. We define the single-node mass distribution $P(m,t)$ at time t, i.e., the probability that a node has mass m at t as
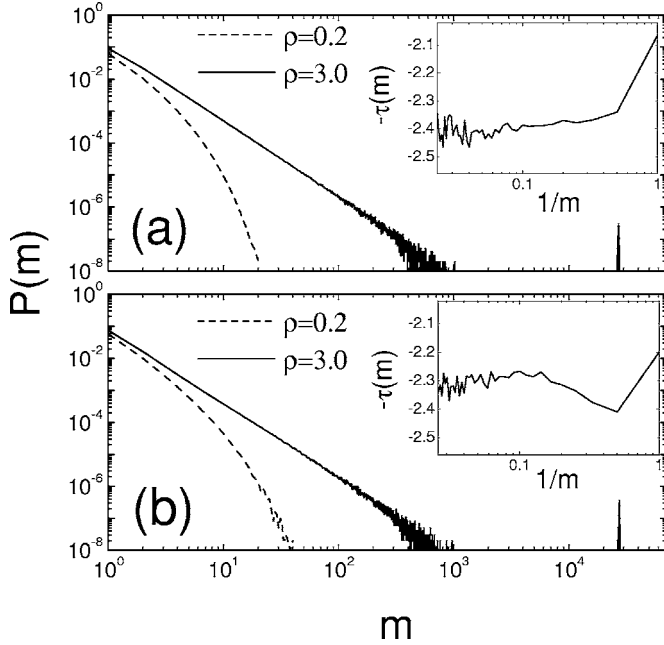
FIG. 2. $P(m)$ on RN (a) and SFN with $\gamma=4.3$ (b) at $\omega=1.0$. In each panel, the solid and the dashed line correspond to $P(m)$ of $\rho=3.0$ (condensed phase) and 0.2 (fluid phase), respectively. The inset in each panel shows the effective exponent $\tau(m)\{\equiv-\ln[P(bm)/P(m)]/\ln b\}$.

$$P(m,t) = \frac{1}{N}n(m,t) = \frac{1}{N}\sum_{i=1}^{N}\delta_{m_i(t),m}, \qquad (2)$$

where $n(m,t)$ is the number of nodes with mass m at time t and $m_i(t)$ is the mass of node i at t. From the conservation of total masses and the normalization condition of $P(m,t)$, i.e., $\Sigma_m P(m,t)=1$, all $P(m,t)$ are expected to reach the stationary state at the same time. For instance, let $P(m_o,t)$ reach the steady state at time τ_o. Then $P(m_o)[=P(m_o,t>\tau_o)]$ is given as $P(m_o)=1-\Sigma_{m\neq m_o}P(m,t)$ after $t\geq\tau_o$. The sum is constant, and each $P(m,t)$ in the sum is also expected to be a constant. Otherwise, for example, the time dependence of $P(m_o\pm1,t)$ in the sum would lead to the change of $P(m_o,t)$ in time. If $P(m_o-1,t)$ is in the steady state, then $P(m_o-2,t)$ is also in the steady state. Since all masses are correlated in this hierarchical manner due to the conservation of total masses, the time dependence of any $P(m,t)$ would lead to the change of the sum in time. So the characteristic time τ_m at which $P(m,t)$ saturates is expected to be independent of mass m, and

$$\tau_0 = \tau_1 = \cdots = \tau_{m^*}, \qquad (3)$$

where m^* is the maximal mass. In Fig. 1, we plot $P(m,t)$ of $m=1$ and 10 for $\omega=1.0$ and $\rho=0.2$ on various networks. The vertical dotted line denotes the characteristic time τ_m, which supports Eq. (3). We also check $P(m,t)$ of various masses up to $m=300$, and find that all $P(m,t)$ reach the steady state nearly at the same time.

We measure the steady-state distribution $P(m)$ by averaging $P(m,t)$ after τ_m. Figure 2 shows the plots of $P(m)$ versus
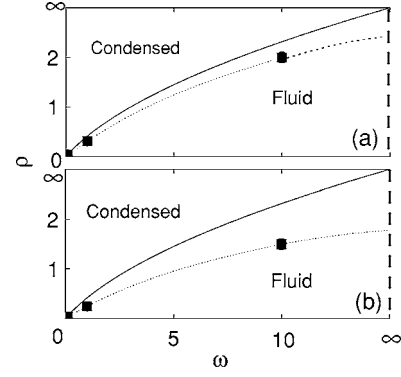

FIG. 3. The ρ-ω phase diagram of RN (a) and SFN with $\gamma=4.3$ (b). In each panel, the solid line is the critical line of $\rho_c(\omega)=\sqrt{\omega+1}-1$ on regular lattices of Ref. [13]. The dotted line between data points is a guide to the eye. The dashed line denotes $\omega=\infty$ line.

m for RN and SFN with $\gamma=4.3$ with $\omega=1.0$. We estimate the critical density ρ_c as $\rho_c(\omega=1)=0.31(3)$ for RN and 0.24(3) for SFN with $\gamma=4.3$, respectively, by examining when the condensation disappears. In fluid phase ($\rho<\rho_c$), $P(m)$ exponentially decays for large mass in both RN and SFN with $\gamma=4.3$. For the condensed phase ($\rho\geq\rho_c$), $P(m)$ algebraically decays on both RN and SFN with $\gamma=4.3$ as $P(m)\sim m^{-\tau}$ with one common τ. For the estimate of τ, we investigate the effective exponent $\tau(m)$ defined by $\tau(m)\equiv-\ln[P(bm)/P(m)]/\ln b$ with $b=2$ at $\rho=3.0$ (Fig. 2). We estimate $\tau=2.40(4)$ for RN from $\tau(m)$ for the range $17\leq m\leq46$ in the inset of Fig. 1(a). Similarly, we find $\tau=2.32(5)$ for SFN with $\gamma=4.3$ from $\tau(m)$ for the range $18\leq m\leq45$ in the inset of Fig. 2(b). The numerical value in the one-dimensional lattice has been reported as $\tau=2.33(2)$ [13]. Hence the values of τ for both networks also reasonably agree with $\tau=5/2$ of regular lattices [13,14]. In condensed phase ($\rho=3.0>\rho_c$), the access mass of $(\rho-\rho_c)N\approx2.7\times10^4$ condenses on a single node in both networks without changing the background critical distribution. To map out phase diagrams for RN and SFN with $\gamma=4.3$, we measure ρ_c and τ for $\omega=0.1, 1.0$, and 10, and find that τ is the same within error on the critical line. Figure 3 shows the phase diagrams of RN and SFN with $\gamma=4.3$. The solid line denotes the critical line, $\rho_c=\sqrt{\omega+1}-1$, of regular lattices [13]. On regular lattices, the $\rho_c(\omega)$ is independent of dimensionality. However on networks, $\rho_c(\omega)$ depends on the underlying network structures. We also confirm that SFN with $\gamma=3.5$ undergoes the same type of condensation transitions. Therefore, we conclude that the SCA model on RNs and SFNs with $\gamma>3$ undergoes the same type of condensation transitions from fluid phase into condensed phase for $0<\omega<\infty$ as those on a one-dimensional regular lattice. However, the critical line depends on the underlying network structures [20,21].

IV. SCA MODEL ON SFN WITH $2\leq\gamma\leq3$

For $\omega\neq\infty$, we perform simulations on SFNs with $\gamma=2.4$ and 3 with $N=10^4$ nodes and $K=2\times10^4$ links. We plot
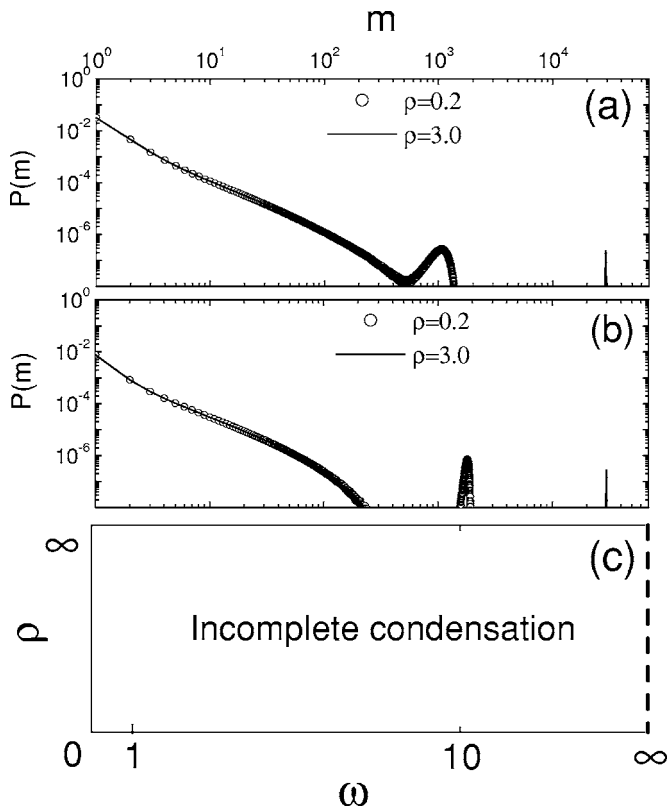
FIG. 4. $P(m)$ on SFN with $\gamma=3$ (a) and $\gamma=2.4$ (b) at $\omega=1.0$. In each panel, the solid and the dashed line correspond to $P(m)$ of $\rho=3.0$ and 0.2, respectively. (c) The typical phase diagram of SFNs with $\gamma \leq 3$. The dashed line denotes the line of $\omega=\infty$.

$P(m,t)$ of $\gamma=2.4$ in Fig. 1(c) for example, and average $P(m,t)$ after τ_m for the steady state $P(m)$. As mentioned in the previous section, τ_m is the same for all masses.

The mass distribution $P(m)$ for $\gamma \leq 3$ shows quite different behavior from that for $\gamma > 3$. Figure 4 shows $P(m)$ on SFNs with $\gamma=2.4$ and 3 for $\rho=0.2$ and 3.0 with $\omega=1$. As in the condensed phase of RNs and SFNs with $\gamma > 3$, there is a condensation of mass $m^* \approx \rho N$. However, $P(m)$ exponentially decays for large m rather than power-law. We also measure $P(m)$ for various ω and ρ, and confirm the same behavior of $P(m)$. Therefore, we conclude that for $\omega \neq \infty$, SCA on SFNs with $\gamma \leq 3$ exhibits an infinite aggregation with an exponential background mass distribution. We call this phase the incomplete condensed phase to reflect exponential mass distributions [Fig. 4(c)]. Intriguingly, the two features of the fluid and the condensed phase on a regular lattice coexist on SFNs with $\gamma \leq 3$. Such a behavior was found in the lattice gas model proposed to describe the distribution of droplets in the fragmentation process following a nuclear collision [22].

The nonexistence of the fluid phase for $\gamma \leq 3$ mainly comes from the hub structure of SFNs with $\gamma \leq 3$ where one or several nodes have a finite fraction of total links [5]. Due to the hub structure, all masses move to a hub node by both diffusion and chipping processes, unlike SFNs with $\gamma > 3$ where the chipping tends to split masses and prevents aggregations. Hence there are no processes to prevent the formation of infinite aggregation for $\gamma \leq 3$. The difference from

ZRP is that the diffusion process moves an infinite aggregation of mass m_{hub} at a hub node to the others. Then the chipping distributes small masses of m_{hub} onto neighboring nodes. In this way, nodes with small degree can have mass so the resultant $P(m)$ is exponential.

Recently, another aggregation-chipping model was studied in which there is no translational invariance [27]. In the model, at any site except origin, all the mass at that site moves as a whole to one of the nearest-neighboring sites with rate 1 and it coalesces with the mass already presents on the neighboring site instantaneously. At the origin, only a single monomer chips off at rate w leaving the rest of the mass behind. For isotropic chipping, the system is in the so-called unpinned aggregate (UA) phase where more than one infinite aggregate coexist. One infinite aggregate presents at the origin and the others move around bulk sites. However, the aggregate at the origin can disintegrate and re-form due to the nonzero probability of zero mass at the origin. Hence the origin is occupied only for a finite fraction of time by an infinite aggregate [27]. However, in the SCA model on SFNs with $\gamma \leq 3$, the condensation occurs due to the strong inhomogeneity of networks, i.e., hub structure. Once the condensate is formed at a hub, it moves around by the diffusion process, as we shall show in Fig. 6(b). By chipping process, the moving condensate may lose masses, but it gains masses at a hub again. Hence the disintegration and the finite occupation time are not expected in SFN with $\gamma \leq 3$.

It is hard to show the existence of infinite aggregation for the limit of $\rho \to 0$ numerically with finite-size networks. Instead we investigate annihilating random walks of two particles on SFNs (lamb-lion problem) for the condition of the existence of the fluid phase on SFNs. For the $\rho \to 0$ limit, we assume an infinite aggregation and neglect the presence of other masses. Then unit mass chips off from the aggregation, and diffuses around on the networks. For the existence of an infinite condensate in the steady state, the two masses should aggregate again in the finite-time interval. If not, unit mass continuously chips off from the infinite aggregation, which will finally disappear. Hence if the unit mass (lamb) survives indefinitely without meeting the infinite aggregation (lion), then the fluid phase exists at the zero density limit. Otherwise, the condensed phase exists for any $\rho > 0$. In the next section, we investigate a lamb-lion problem on RNs and SFNs.

V. LAMB-LION PROBLEM ON NETWORKS

We consider one lamb and one lion problem on networks. If a lamb meets a lion on the same node, then it dies. Hence the interesting quantity is the survival probability $S(t)$ of a lamb at time t. On a d-dimensional regular lattice, $S(t)$ depends on d as follows [23–26]:

$$S(t) \sim \begin{cases} t^{d/2-1} & \text{for } d < 2, \\ 1/\ln t & \text{for } d = 2, \\ \text{const} & \text{for } d > 2. \end{cases} \quad (4)$$

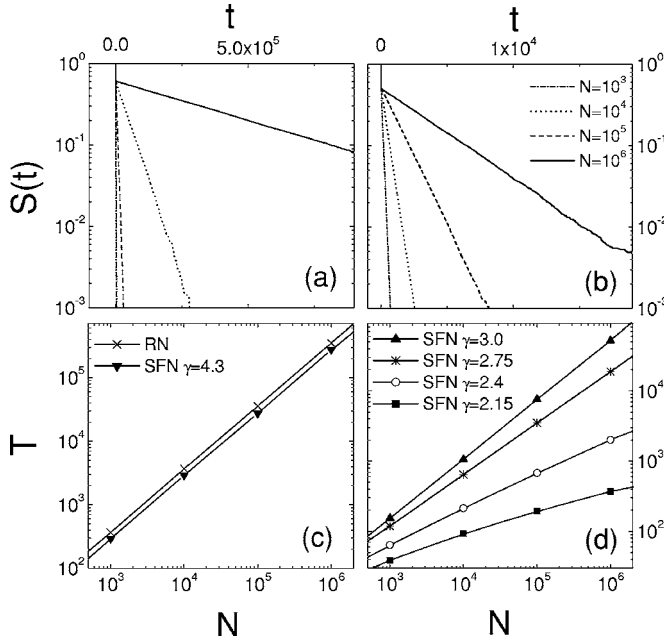On networks, the steady-state distribution of a random walker is proportional to the degree k_i of node i [19] as

FIG. 5. Semilog plot of the survival probability $S(t)$ on SFN with $\gamma=4.3$ (a) and 2.4 (b) of various size N up to 10^6. (c) The average lifetime T on RN and SFN with $\gamma=4.3$. (d) T on SFNs with $\gamma \leq 3$. The solid line between data points is a guide to the eye.

$$P_i^\infty = k_i / \sum_{j=1}^{N} k_j. \tag{5}$$

Hence the probability of finding two walkers at the same node should depend on the second moment $\langle k^2 \rangle$. While $\langle k^2 \rangle$ is finite for RNs and SFNs with $\gamma > 3$, it diverges for SFNs with $\gamma \leq 3$. So RNs and SFNs with $\gamma > 3$ correspond to an infinite dimensional homogeneous regular lattice in macroscopic scale, while SFNs with $\gamma \leq 3$ are generically inhomogeneous. Therefore, $S(t)$ is expected to be constant in the thermodynamic limit on RNs and SFNs with $\gamma > 3$. It means the existence of the fluid phase for the limit of $\rho=0$ for any $\omega \neq \infty$ as shown in Fig. 3. On the other hand, for the incomplete condensed phase of $\gamma \leq 3$, $S(t)$ should decay to zero for $\gamma \leq 3$.

We measure $S(t)$ of a lamb on RNs and SFNs with various γ for several values of N from 10^3 to 10^6 and up to 10^6 time steps. Initially a lamb and a lion are placed on two randomly selected nodes. In Fig. 5, we plot $S(t)$ for $\gamma=4.3$ (a) and 2.4 (b) for various system size N. Interestingly $S(t)$ decays exponentially in both SFNs for any N. For example, $S(t)$ of $\gamma=4.3$ and $N=10^6$ exponentially decays with very large characteristic time τ order of 10^6 over the whole time interval. We also confirm the same exponential decay of $S(t)$ on RNs for any N. Unlike on regular lattices where the exponential decay of $S(t)$ comes from the finite-size effect of lattices, $S(t)$ on networks shows such an exponential decay at very early time. The exponential decay of $S(t)$ mainly comes from the small world nature of networks [5], i.e., the average path length between a pair of nodes increases logarithmically with N. As $S(t)$ shows the exponential decay for any γ, we are interested in the average lifetime T of a lamb rather than $S(t)$ itself.

We measure the lifetime T of a lamb on RNs and SFNs with several γ values for N up to 10^6 and plot T against N in Figs. 5(c) and 5(d). In Fig. 5(c), T linearly increases with N for both RN and SFN with $\gamma=4.3$. Assuming $T \sim N^\alpha$, we estimate $\alpha=1.0(2)$ for RN and SFN with $\gamma=4.3$ by measuring slopes. However, for $\gamma < 3$ of Fig. 5(d), T exhibits quite different behavior. T of $\gamma=2.15$ and 2.4 tend to saturate to some asymptotic value with decreasing successive slopes. However, the characteristic size $N_s(\gamma)$ at which T begins to saturate increases as γ approaches $\gamma=3$. For example, T of $\gamma=2.75$ seems to algebraically increase up to $N=10^6$. It means that N_s of $\gamma=2.75$ is already larger than 10^6. To see the saturation at $\gamma=2.75$, big size N much larger than 10^6 is needed but it is practically very difficult. It is hard to believe that T diverges in power-law fashion as γ approaches 3 because T of small γ has already begun to saturate at moderate N order of $10^5 \sim 10^6$. Hence T of $\gamma < 3$ is expected to saturate to its asymptotic value even though we cannot see the saturation via simulations as γ approaches 3 from below. At $\gamma=3$, T also increases algebraically with N. By measuring successive slopes, we estimate $\alpha=0.85(1)$ for $\gamma=3$. However, as the exponent α continuously varies as γ increases to 3, the value of α at $\gamma=3$ may have no special meaning. As shown in Fig. 4(a) for $\gamma=3$, the condensation already occurs at sufficiently low density $\rho=0.2$ even for small size $N = 10^4$. So T of $\gamma=3$ is believed to saturate in the thermodynamic limit as for $\gamma=2.75$. Therefore, we are convinced that the lifetime of a lamb is finite in the thermodynamic limit $N \to \infty$ for $\gamma \leq 3$. From the behavior of the lifetime T, the asymptotic behavior of $S(t)$ is investigated in the following.

As shown in Fig. 5(a), $S(t)$ decays exponentially as $S(t) = S_o e^{-t/\tau}$. From the definition of $T = \int_0^\infty t[-dS(t)/dt]dt$, we have $T \sim \tau$. Hence τ diverges linearly on SFNs with $\gamma > 3$ and RNs, while it saturates for $\gamma \leq 3$. The scaling behavior of τ means that $S(t)$ on RNs and SFNs with $\gamma > 3$ is nonzero constant in the limit $N \to \infty$, and exponentially decays to zero on SFNs with $\gamma \leq 3$. Hence we have

$$\lim_{N \to \infty} S(N,t) = \begin{cases} S_o e^{-t/\tau_\infty} & (\gamma \leq 3) \\ S_\infty & (\gamma > 3), \end{cases} \tag{6}$$

where τ_∞ is the asymptotic value of τ, and depends on γ. As $S(t)$ decays exponentially to zero for $\gamma \leq 3$, two particles initially located on the same node should meet or aggregate within a finite time interval. Hence the finite lifetime on SFNs with $\gamma \leq 3$ supports the numerically expected condensed phase for any $\rho > 0$ on SFNs with $2 \leq \gamma \leq 3$ as mentioned in the previous section. On the other hand, the finite S_∞ on RNs and SFNs with $\gamma > 3$ implies the existence of the fluid phase in the limit $\rho \to 0$, which is also consistent with the phase diagrams of Fig. 3.

VI. SCA MODEL AT $\omega = \infty$

At $\omega = \infty$, the SCA model corresponds to ZRP with constant hopping rate on networks. On SFNs with $\gamma > 2$, it was shown that ZRP undergoes complete condensation for any
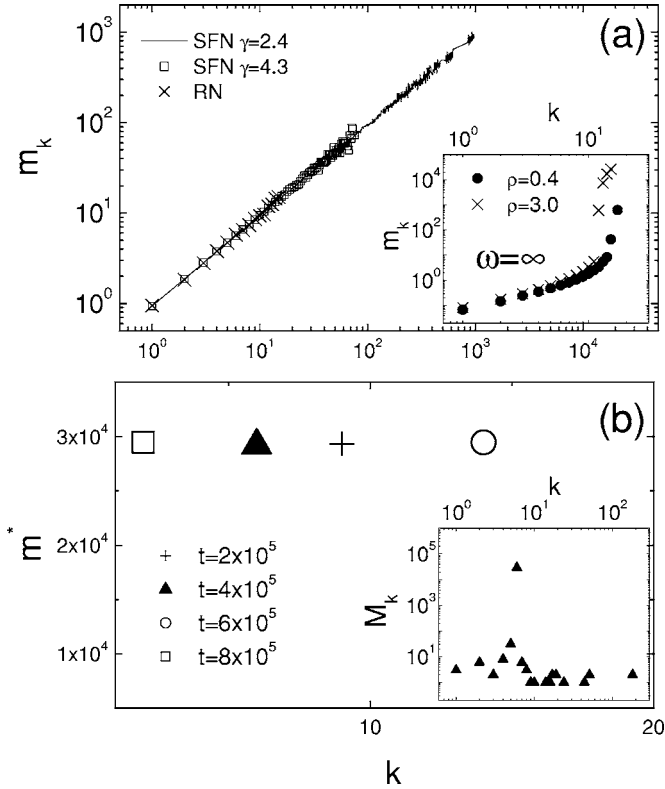
FIG. 6. (a) The main plot shows m_k of Eq. (10) for $\rho=3.0$ and $\omega=1$ on RN, SFN with $\gamma=4.3$ and 2.4 in condensed phase. The inset shows m_k at $\omega=\infty$ on RN. (b) M_k of a single sample on SFN with $\gamma=2.4$ at different times for $\rho=3$ and $\omega=1$ of the condensed phase. The main plot only shows the maximum mass m^* of M_k of a single sample at different time steps, and the inset shows the snapshot of the M_k at $t=4\times10^5$.

$\rho>0$ [6]. In condensation phenomena of ZRP on SFNs, the average mass at a node with degree k, m_k in the steady state exhibits a discontinuous jump at a hub node. In ZRP with constant chipping rate, for example, m_k linearly increase until $k<k_{hub}$ and jumps to the value $m^*\approx\rho N$ at $k=k_{hub}$ [6]. The k_{hub} is the degree of the hub node which has the largest number of links.

To see whether the condensation occurs on RNs in ZRP, we measure m_k for $\rho=0.4$ and 3.0 on RNs with $N=10^4$. As shown in the bottom inset of Fig. 6(a), m_k increases linearly in k and finally jumps at k_{hub} as in ZRP on SFNs. For a fixed N, the mass of k_{hub}, m_{hub} decreases as ρ goes to zero, as shown in the inset of Fig. 6(a). So it is hard to observe the condensation at low density for small N. Since the complete condensation of ZRP on networks mainly comes from the inhomogeneity of degree distribution rather than the competition between dynamical processes, ZRP on RNs should exhibit the complete condensation for any $\rho>0$ as on SFNs. At $\omega=\infty$, we also measure m_k on SFNs with $\gamma\leq3$ and confirm the complete condensation as shown in Ref. [6]. Together with the recent study on SFNs [6], the complete condensation always occurs on both RNs and SFNs in the zero range process with constant hopping rate.

The discontinuity of m_k clearly comes from the nature of the chipping process of unit mass. That is, unit mass hops

around according to the steady-state distribution of Eq. (5), and then there is enough net particle current into the hub nodes to form infinite aggregation. However, when the diffusion of the whole mass of each node turns on, the aggregation at the hub node diffuses around all nodes. The diffusion of the condensate completely changes the behavior of m_k in the condensed phase of finite ω. m_k linearly increases up to k_{hub} without any jump in the condensed phase of $\omega \neq \infty$. In the next section, we numerically and analytically confirm the linearity of m_k in k.

VII. AVERAGE MASS OF A NODE WITH DEGREE k

Another interesting quantity in condensation phenomena on networks is the average mass at a node with degree k, m_k in the steady state. In ZRP with chipping rate $u(m)\sim m^\delta$ on SFNs [6], the complete condensation takes place for $\delta<\delta_c=1/(\gamma-1)$. For $\delta<\delta_c$, m_k linearly increases with k for $k \ll k_c$, and algebraically increases as $k^{1/\delta}$ for $k\geq k_c$. Especially at $\delta=0$, m_k linearly increases until $k<k_{hub}$ and jumps to the value $m^*\approx\rho N$. The k_{hub} is the degree of the hub node which has the largest number of links. The same type of behavior on RN for $\omega=\infty$ is shown in the inset of Fig. 6(a).

In the SCA model, as all masses can perform random walks according to the steady-state distribution P_i^∞ of Eq. (5), one can expect the jump of m_k at k_{hub} in the condensed phase for $\omega\neq\infty$ in the SCA model as in ZRP. However, as shown in the main plot of Fig. 6(a), m_k increases linearly in k up to k_{hub} and there is no jump, unlike in ZRP. In Fig. 6(a), we plot m_k versus k for $\rho=3.0$ and $\omega=1.0$, which corresponds to the condensed phase of both RN and SFN with $\gamma=4.3$. We also measure m_k in the fluid phase ($\rho=0.2, \omega=1.0$) of both networks (not shown), and confirm $m_k\sim k$ without any jumps. For SFN with $\gamma=2.4$, m_k also shows the linearity in k for $\rho=3.0, \omega=1.0$. Our simulation results imply that the relation $m_k\sim k$ is valid for any $\rho>0$ in RNs and SFNs with $\gamma\geq2$ for finite diffusion rate. The diffusion of masses indeed results in the linearity of m_k in k for any $\omega\neq\infty$.

In the steady state, as masses can perform random walks with a finite rate, the mass of a hub node (m_{hub}) diffuses to different nodes with the probability of being at node i given as Eq. (5) [19]. The inset of Fig. 6(b) shows the snapshot of the mass distribution of nodes with degree k for a single sample at time $t=4\times10^5$ on SFN with $\gamma=2.4$ for $\rho=3.0$ and $\omega=1.0$. As shown, there is a peak which may be formed at k_{hub} as in ZRP. However, the peak of mass m^* is not always located at k_{hub} but diffuse around nodes according to P_i^∞ [Fig. 6(b)]. Hence by taking the average, the peak soaks into the average mass m_k, unlike in ZRP where all samples have the peak at k_{hub}. To see this more explicitly, we derive the relation, $m_k\sim k$, based on the assumption that the diffusion (the random walks of masses) is the only relevant physical factor to decide $P(m)$ in the steady state.

First, we consider the average total mass M_k of nodes with degree k defined as

$$M_k = \sum_{m=0}^{\infty} mP_\infty(m,k), \qquad (7)$$

where $P_\infty(m,k)$ is the probability of finding a random walker with mass m at degree k in the steady state. As mass distri-

bution $P(m)$ in the steady state is independent of k, we have $P_\infty(m,k)=P(m)P_k^\infty$. P_k^∞ is the probability of finding a random walker at a node with degree k on the network. Then using P_i^∞ of Eq. (5), we write P_k^∞ as

$$P_k^\infty = \sum_{i=1}^{N} P_i^\infty \delta_{k_i,k} = \frac{kNP(k)}{\sum_{j=1}^{N} k_j}, \qquad (8)$$

where $P(k)$ is a degree distribution. From Eqs. (7) and (8), we have

$$M_k = \left[\frac{kNP(k)}{\sum_{j=1}^{N} k_j}\right]\left[\sum_{m=0}^{\infty} mP(m)\right]. \qquad (9)$$

So $M_k = \bar{m}kP(k)/\langle k \rangle \sim kP(k)$. Then the average mass of a node with degree k is given as

$$m_k = \frac{M_k}{NP(k)} \sim k/N. \qquad (10)$$

As expected, m_k scales as $m_k \sim k$ for any degree distribution $P(k)$. As Eq. (10) is valid for any density $\rho > 0$, m_k does not undergo the condensation transitions, unlike $P(m)$ of Eq. (1). Therefore, the steady-state distribution of m_k is determined by diffusion of masses rather than chipping of unit mass, unlike in ZRP.

VIII. SUMMARY

We investigate the condensation phase transitions of the symmetric conserved-mass aggregation (SCA) model on networks. In the SCA model, masses diffuse with unit rate, and unit mass chips off from mass with rate ω. The SCA model undergoes condensation phase transitions via the competition between diffusion and chipping processes [13].

First we consider the $\omega \neq \infty$ case. On random and scale-free networks of $\gamma > 3$, the SCA model undergoes the same type of condensation transitions from fluid phase into condensed phase as in the one-dimensional lattice of Ref. [13]. However, unlike on regular lattices, the critical line on the networks depends on the network structures. On the other hand, on scale-free networks of $\gamma \leq 3$ where one or several nodes have a finite fraction of degrees, an infinite aggregation with exponentially decaying background mass distribution always takes place for any nonzero density, so no phase transitions occur for $\omega \neq \infty$. The condensation and exponential mass distribution of small masses come from the generic

inhomogeneity of network structure of SFNs with $\gamma \leq 3$. However, we are not able to numerically show the existence of the condensation phase at the zero density limit for $\gamma \leq 3$ due to the small world nature of networks [5]. Instead, we numerically study the survival probability of particle in pair annihilating random walks, the so-called one lamb and one lion problem on networks.

For the formation of an infinite aggregation of masses at the zero density limit, unit mass chipped off from the infinite aggregation should aggregate again with the aggregation within the finite time interval. We numerically show that in the thermodynamic limit, the survival probability $S(t)$ of a lamb (unit mass) is finite on random networks and scale-free networks (SFNs) with $\gamma > 3$, but exponentially decays to zero with finite lifetime on SFNs with $\gamma \leq 3$. Based on the finite lifetime of a lamb on SFNs with $\gamma \leq 3$, we indirectly confirm the incomplete condensed phase for any $\rho > 0$ on SFNs with $\gamma \leq 3$.

At $\omega = \infty$, the SCA model corresponds to the zero-range process (ZRP) with constant chipping rate [1]. ZRP with constant chipping rate on SFNs was shown to exhibit complete condensation [6]. We also numerically show that the complete condensation takes place for any $\rho > 0$ on random networks by measuring the average mass of a node with degree k. Hence the complete condensation always takes place for any nonzero density in ZRP with constant chipping rate on random and scale-free networks.

Finally, we investigate the behavior of the average mass of a node with degree k, m_k in the fluid and the condensed phase. In ZRP with constant chipping rate, m_k linearly increases with degree k, and jumps to the total mass of the system at hub degree k_{hub} [6]. Hence in the SCA model, m_k is expected to show such a jump in the condensed phase for $\omega \neq \infty$. However, m_k linearly increases up to k_{hub} without jumps in both the fluid and the condensed phase. We numerically confirm the linearity of m_k, and also analytically show $m_k \sim k$ with the assumption that the diffusion is the only relevant factor in the steady state. Therefore, the steady-state distribution of m_k is determined by diffusion of masses rather than chipping of unit mass, unlike in ZRP.

[1] M. R. Evans, Braz. J. Phys. **30**, 42 (2000); M. R. Evans and T. Hanney, J. Phys. A **38**, R195 (2005).

[2] M. R. Evans, Europhys. Lett. **36**, 13 (1996).

[3] O. J. O'Loan, M. R. Evans, and M. E. Cates, Phys. Rev. E **58**, 1404 (1998).

[4] D. van der Meer *et al.*, J. Stat. Mech.: Theory Exp. 2004, P04004; J. Torok, e-print cond-mat/0407567.

[5] S. N. Dorogovtsev and J. F. F. Mendes, Adv. Phys. **51**, 1079 (2002); R. Albert and A.-L. Barabási, Rev. Mod. Phys. **74**, 47 (2002).

[6] J. D. Noh, G. M. Shim, and H. Lee, Phys. Rev. Lett. **94**, 198701 (2005).

[7] A. G. Angel, T. Hanney, and M. R. Evans, e-print cond-mat/0509238.

[8] R. M. Ziff, J. Stat. Phys. **23**, 241 (1980).

[9] W. H. White, J. Colloid Interface Sci. **87**, 204 (1982).

[10] A. E. Scheidegger, Bull. I.A.S.H. **12**, 15 (1967).

[11] A. Maritan, A. Rinaldo, R. Rigon, A. Giacometti, and I. Rodriguez-Iturbe, Phys. Rev. E **53**, 1510 (1996); M. Cieplak, A. Giacometti, A. Maritan, A. Rinaldo, I. R. Iturbe, and J. R. Banavar, J. Stat. Phys. **91**, 1 (1998).

[12] S. K. Friedlander, *Smoke, Dust and Haze* (Wiley Interscience, New York, 1977).

[13] S. N. Majumdar, S. Krishnamurthy, and M. Barma, Phys. Rev. Lett. **81**, 3691 (1998); J. Stat. Phys. **99**, 1 (2000).

[14] R. Rajesh and S. N. Majumdar, Phys. Rev. E **63**, 036114 (2001).

[15] R. Rajesh and S. Krishnamurthy, Phys. Rev. E **66**, 046132 (2002).

[16] R. Rajesh, D. Das, B. Chakraborty, and M. Barma, Phys. Rev. E **66**, 056104 (2002).

[17] A. V. Goltsev, S. N. Dorogovtsev, and J. F. F. Mendes, Phys. Rev. E **67**, 026123 (2003).

[18] K.-I. Goh, B. Kahng, and D. Kim, Phys. Rev. Lett. **87**, 278701 (2001).

[19] J. D. Noh and H. Rieger, Phys. Rev. Lett. **92**, 118701 (2004).

[20] H. Takayasu, I. Nishikawa, and H. Tasaki, Phys. Rev. A **37**, 3110 (1988); H. Takayasu, Phys. Rev. Lett. **63**, 2563 (1989).

[21] R. Rajesh and S. N. Majumdar, Phys. Rev. E **63**, 036114 (2001).

[22] X. Campi and H. Krivine, Nucl. Phys. A **620**, 46 (1997).

[23] M. Bramson and D. Griffeath, Capture Problems for Coupled Random Walks, in *Random Walks, Brownian Motion, and Interacting Particle Systems: A Festschrift in Honor of Frank Spitzer*, edited by R. Durrett and H. Kesten (Birkhauser, Boston, 1991), pp. 153–188.

[24] W. Feller, *An Introduction to Probability Theory* (Wiley, New York, 1971), Vol. 1.

[25] *Aspects and Applications of the Random Walk* (North-Holland, Amsterdam, 1994).

[26] P. L. Krapivsky and S. Redner, J. Phys. A **29**, 5347 (1996).

[27] K. Jain and M. Barma, Phys. Rev. E **64**, 016107 (2001).